Yan et al. 2017. *Int. J. Vehicle Structures & Systems*, 9(4), 206-211
ISSN: 0975-3060 (Print), 0975-3540 (Online)
doi.org/10.4273/ijvss.9.4.01

International Journal of Vehicle Structures & Systems
Available online at www.maftree.org/eja

Acceleration Analysis of Tubular Constrained Damping Engine Mount

Bijuan Yan[a], Baoxiang Lang, Zhangda Zhao and Dagang Sun

School of Mech. Engg., Taiyuan University of Sci. & Tech., Taiyuan, Shanxi, China
[a]Corresponding author, Email : s2003110@126.com

ABSTRACT:

Trackless vehicles have been widely used for the underground mining in many coal-rich countries. However, their vibration is violent and this vibration could affect the driver's health and reduce the working efficiency. Therefore, how to solve this question about the vibration and shock has become an urgent and important thing. In this paper, a type of tubular constrained damping engine mount is designed and first used in the underground trackless vehicles. This tubular damping structure is made of three layers, the external and internal layer are made of steel and the middle layer of natural rubber is sandwiched between them. To know about the vibration-reducing performance of the new designed mounts, the real vehicle test was performed under two working conditions. The results show that the two rear mounts could obtain good vibration isolation effect, whereas the performance are sometimes poor in a certain direction for the two front mounts because of the vibration energy coupling in different directions. Further research is to optimize the parameters of the tubular constrained damping engine mount to make the vibration energies from different directions decoupled.

KEYWORDS:

Underground trackless vehicle; Tubular structure; Engine mount; Constrained damping

CITATION:

B.J. Yan, B.X. Lang, Z.D. Zhao and D.G. Sun. 2017. Acceleration Analysis of Tubular Constrained Damping Engine Mount, *Int. J. Vehicle Structures & Systems*, 9(4), 206-211. doi:10.4273/ijvss.9.4.01

1. Introduction

Trackless vehicles have been widely used in many coal-rich countries because their applications not only improve the mine productivity and transportation efficiency, but also provide guarantee for safe production of underground mining [1]. However, these vehicles often run and work in the underground for a long time and vibration and shock are inevitable which mainly come from two parts: the uneven road and the working engine. As is well known, the vibration could affect the driver's health and reduce the working efficiency, and on the other hand, the service life of the vehicles' parts will also be dropped [2-3]. So it becomes an important problem that how to reduce the vibration of underground trackless vehicles and improve their market competitiveness. As above mentioned, the engine is one of the major vibration sources because the unbalanced disturbance forces may occur during its operating. So, various engine mounts become necessary and important in the control activities of vehicle's vibration and shock.

Here, it is noted that the mounts should not only have the ability to support the engine's weight, and their main function is to isolate the engine-induced vibration from the chassis [4]. In order to reduce the vibration level of the whole vehicle, passive, semi-active and active control technologies have been applied during the design process of engine mounts [5]. For example, passive rubber damping engine mounts have been successfully used in the vehicles for many years. Now, the types of rubber isolator are expanding to meet various demands. Östberg et al designed a kind of hollowed cylindrical rubber vibration isolators which consisted of rubber and metal elements in series [6]. At the same time, passive hydraulic engine mounts were employed by the automotive manufacturer in the mid-1980s to obtain an increase of damping and comfort levels [7-8]. Afterwards, semi-active and active vibration control techniques were developed by many researches [9-10]. In the semi-active engine mounts, the damping or more system parameters could be varied by the use of sensors and actuators.

Besides sensors and actuators, active methods also use additional electronics and fluids to achieve better control performance [11]. Through comparison among passive, semi-active and active control methods, it may be found that the semi-active and active will bring out some problems such as the additional system weight, high cost and energy demands [12]. More importantly, although many engine mounting vibration-reducing technologies have received good isolation effects, much attentions are still only concentrated in the automotive, marine and aircraft applications [13-14]. In other words, the take up of the vibration-reducing technology is somewhat slow in the underground trackless vehicles. There are many kinds of underground trackless vehicles in China [15]. In this paper, one of them Fig. 1a is taken as the research object. At present, this type of vehicle is only equipped with the conventional engine mounts Fig. 1b, which only give effective vibration isolation along one degree of freedom.

Fig. 1(a): Photo of underground trackless vehicle

Fig. 1(b): Conventional old engine mount

Over time and use, these mounts begin to tear and fail to work normally during their service time. And this will change the height and position of the engine, which not only causes a deteriorating riding, but also has a risk to destroy the other components. From above analysis, it is known that it is necessary and vital to improve the performance of the existing engine mounts used for these underground vehicles. To this end, a kind of tubular constrained damping engine mount which is also called tubular sandwiched engine mount is designed and first used in the underground trackless vehicles. The related real vehicle tests are performed to check the vibration-reducing effects of this new mount. This research is helpful to grasp the actual application of the tubular sandwiched structure and further improve the comfort performance of the underground trackless vehicles.

2. Tubular constrained damping engine mount

2.1. Parameters and vibration characteristics of diesel engine

Based on the characteristics of diesel engine such as high fuel efficiency, heavy duty, strong dynamic performance and good economic performance, there are many large on and off road construction and mine vehicles which are installed with diesel engine as a power source. With the developments of trackless mechanized mining, a demand for diesel engine equipments becomes popular. In order to meet the requirements of the special underground working environment, diesel engine must be flame-proof. Table 1 shows some important parameters of a 6-cylinder engine used in this study. There are various factors which contribute to engine's vibration [16]. For the 6-cylinder engine used in the underground trackless vehicle, the crankshaft torsional vibration play an important responsible for the whole engine's vibration. When the crankshaft rotates during operation of engine, the piston goes through 4 different strokes. Thus the speed fluctuations and the periodic variation of pulse torque output of crankshaft could exist. As a result, it will cause engine's periodic torsional vibration. In addition, it should be pointed out that unbalanced inertia force of six cylinder engine and unbalanced inertia torque can be completely balanced due to its structure.

Table 1: Main parameters of diesel engine

Name	Value
No. of cylinders	6
Cycle	4-stroke
Special demand	Flame-proof
Mass	550kg
Output power	92kW
Idle speed	600r/min
Speed range	1500r/min~2300r/min

2.2. Tubular engine mount

2.2.1. Structure of tubular constrained damping engine mount

Structure of tubular constrained damping engine mount is shown in Fig. 2. From Fig. 2, it could be well known that the mount uses a kind of sandwiched structure. The external and internal layers are made of steel and the external layer is often called the constrained layer. The middle layer of natural rubber is sandwiched between them. Three layers are bonded together through vulcanization. This production technology has become more and more mature and the mold is also simple, so the manufacture cost is low. For this type of structure, it is symmetry in axial and radial directions, so it can better attenuate the vibration, whereas the old existing engine mount could only get vibration-reducing effect in the vertical direction. In addition, its radial stiffness is relatively large, and it has enough ability to support the engine's mass. Based on these advantages, this tubular sandwiched absorber is chosen as engine mount and its basic parameters are shown in Table 2. Through contrast of three layer's material, it is clear that the rubber's stiffness is relatively lower, therefore, the vibration energy is mainly dissipated through the deformation and hysteresis of natural rubber to achieve the design requirements.

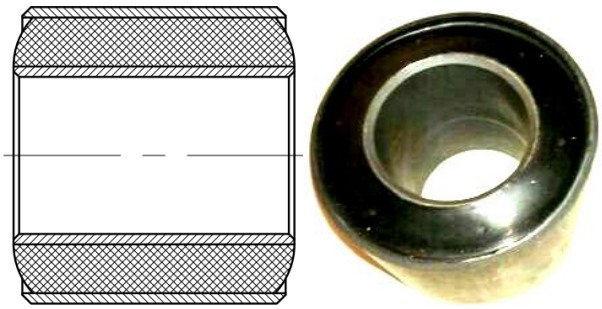

a): Schematic diagram **b): Actual structure**

Fig. 2: Tubular constrained damping engine mount

Table 2: Basic parameters of tubular sandwiched engine mount

Name	Value
Inner diameter of whole mount	45 mm
Outside diameter of whole mount	85 mm
Thickness of steel layer	3 mm
Inner diameter of rubber layer	51 mm
Outside diameter of rubber layer	79 mm
Thickness of rubber layer	14 mm
Total length	80 mm
Total mass	0.259 kg
Rubber hardness	60 (shore A)

2.2.2. Connecting device between engine and tubular constrained damping engine mount

When the tubular sandwiched mount is used in the underground trackless vehicle, its inner layer is connected with the connecting shaft and its outside layer is assembled with the supporting device, which could be seen in the Fig. 3. Here, it should be noted that the connecting shaft is fixed together with the engine by four bolts, and the supporting device is connected with the chassis of the vehicle. The shim is used to adjust the gap between the two parts of the supporting device of mount. Here, four tubular engine mounts are installed at each corner of engine system. In other words, a four-point support way is applied in the engine mount system, which is shown in the Fig. 4.

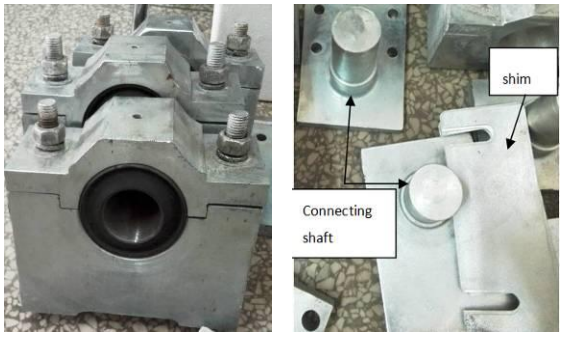

Fig. 3: Supporting device of mount and Connecting shaft and shim

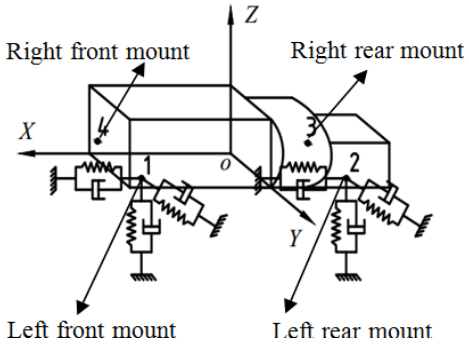

Fig. 4: Layout of engine mount system

3. Mathematical model

Mathematical model of tubular sandwiched engine mount system is established based on the Lagrange Eqn. The Lagrange Eqn. under the conservative system is as follows [17],

$$\frac{d}{dt}\left[\frac{\partial T}{\partial \dot{Q}}\right]-\frac{\partial T}{\partial Q}+\frac{\partial V}{\partial Q}+\frac{\partial D}{\partial Q}=F \tag{1}$$

where T, V and D are total kinetic energy, potential energy and dissipation energy of engine mount system, respectively. F is the excitation force which is exerted on the engine mount system. Q stands for the generalized momentum of the engine mount system, which may be linear momentum, angular momentum or other physical quantities. In this study, the engine and chassis are taken as rigid body, thus, Q is generalized coordinates, and Q = [x, y, z, θ_x, θ_y, θ_z]. Here, x, y, z are the linear moving coordinates and θ_x, θ_y, θ_z are rotary coordinates which are relative to X, Y, Z -axis in Fig. 4, respectively. In the Eqn. (1), the total kinetic energy T could be written as follows,

$$T=T_T+T_R=\frac{1}{2}m\left(\dot{x}^2+\dot{y}^2+\dot{z}^2\right)+\frac{1}{2}\sum_{i=1}^{n}m_i v_i^2 \tag{2}$$

where n is the total number of particles the engine mount system is subdivided into, m_i stands for the mass of the i^{th} particle, v_i is the absolute velocity, the total mass of the engine mount system is m. T_T is the linear moving part of the kinetic energy, T_R is the rotary kinetic energy and can be expressed as,

$$\begin{aligned}T_R=&\frac{1}{2}\sum_{i=1}^{n}m_i v_i^2=\frac{1}{2}\left[\sum_{i=1}^{n}m_i\left(y_i^2+z_i^2\right)\right]\dot{\theta}_x^2+\\&\frac{1}{2}\left[\sum_{i=1}^{n}m_i\left(z_i^2+x_i^2\right)\right]\dot{\theta}_y^2+\frac{1}{2}\left[\sum_{i=1}^{n}m_i\left(x_i^2+y_i^2\right)\right]\dot{\theta}_z^2\\&-\frac{1}{2}\left[\sum_{i=1}^{n}m_i x_i y_i\right]\dot{\theta}_x\dot{\theta}_y--\frac{1}{2}\left[\sum_{i=1}^{n}m_i z_i y_i\right]\dot{\theta}_z\dot{\theta}_y\\&-\frac{1}{2}\left[\sum_{i=1}^{n}m_i x_i z_i\right]\dot{\theta}_x\dot{\theta}_z\end{aligned} \tag{3}$$

Next, the moment of inertia of engine system I_{xx}, I_{yy}, I_{zz} and the product of inertia I_{xy}, I_{yz}, I_{zx} are defined as,

$$\begin{aligned}&I_{xx}=\sum_{i=1}^{n}m_i\left(y_i^2+z_i^2\right),I_{yy}=\sum_{i=1}^{n}m_i\left(z_i^2+x_i^2\right),\\&I_{zz}=\sum_{i=1}^{n}m_i\left(x_i^2+y_i^2\right),\\&I_{xy}=\sum_{i=1}^{n}m_i x_i y_i,I_{yz}=\sum_{i=1}^{n}m_i z_i y_i,I_{zx}=\sum_{i=1}^{n}m_i x_i z_i\end{aligned} \tag{4}$$

Combining Eqns. (2-4) becomes,

$$\begin{aligned}T=T_T+T_R=&\frac{1}{2}m_i x_i^2+\frac{1}{2}m_i y_i^2+\frac{1}{2}m_i z_i^2\\&+\frac{1}{2}I_{xx}\dot{\theta}_x^2+\frac{1}{2}I_{yy}\dot{\theta}_y^2+\frac{1}{2}I_{zz}\dot{\theta}_z^2-\frac{1}{2}I_{xy}\dot{\theta}_x\dot{\theta}_y\\&-\frac{1}{2}I_{yz}\dot{\theta}_z\dot{\theta}_y-\frac{1}{2}I_{zx}\dot{\theta}_x\dot{\theta}_z\end{aligned} \tag{5}$$

The matrix form of Eqn. (5) is given by,

$$\begin{aligned}T=&\frac{1}{2}\left[\dot{x}\,\dot{y}\,\dot{z}\,\dot{\theta}_x\,\dot{\theta}_y\,\dot{\theta}_z\right]\begin{bmatrix}m&0&0&0&0&0\\0&m&0&0&0&0\\0&0&m&0&0&0\\0&0&0&I_{xx}&-I_{xy}&-I_{xz}\\0&0&0&-I_{xy}&I_{yy}&-I_{yz}\\0&0&0&-I_{xz}&-I_{yz}&I_{zz}\end{bmatrix}\begin{bmatrix}\dot{x}\\\dot{y}\\\dot{z}\\\dot{\theta}_x\\\dot{\theta}_y\\\dot{\theta}_z\end{bmatrix}\\=&\frac{1}{2}\dot{Q}^T M\dot{Q}\end{aligned} \tag{6}$$

Then, the total potential energy V could be written as,

$$V=\frac{1}{2}Q^T KQ \tag{7}$$

where K denotes the stiffness matrix of engine mount system and it could be expressed as,

$$K=\sum_{i=1}^{4}B_i^T E_i^T k_i E_i B_i \tag{8}$$

Where $k_i=\begin{bmatrix}k_{ui}&0&0\\0&k_{vi}&0\\0&0&k_{wi}\end{bmatrix}$, k_{ui}, k_{vi}, k_{wi} are the stiffness of three different direction for the tubular sandwiched

engine mount, respectively. B is the position transfer matrix, E is the cosine direction transfer matrix. Similarly, the dissipation energy is given by,

$$D = \frac{1}{2} Q^T C Q \tag{9}$$

where C is the damping matrix of the tubular sandwiched engine mounts. Therefore, by substituting Eqns. (6, 7 and 9) into Eqn. (1), the vibration differential equation of tubular sandwiched engine mount system is resulted as,

$$M\ddot{Q} + C\dot{Q} + KQ = F \tag{10}$$

4. Acceleration analysis

4.1. Test equipment

A real vehicle test was done in order to verify the vibrating-isolating performance of the tubular constrained damping absorbers. Fig. 5 shows a photo of real vehicle test. The DH311E-type accelerometers, charge amplifier and a compute with DH5927 dynamic signal analysis system were used to collect time domain engine vibration signals. For the underground trackless vehicle, there are different working conditions, such as startup, acceleration, braking and cornering and so on. In this paper, vibration response tests were done when the vehicle was operated during the normal driving with a speed of 20km/h and at idle. In other words, only two working conditions are taken into account. Response test schematic of up and down test point vibration is given in Fig. 6. In Fig. 6, four accelerometers are installed under the engine assembly, the other four accelerometers are fixed on the vehicle chassis. Thus, when the engine assembly works, it will produce vibration. These vibration signals which are transmitted from the engine are captured by the four up DH311E-type accelerometers. Simultaneously, the other four down accelerometers are used to receive acceleration signals transmitted to the bottom of the mounts. Because these test vibration signals are very small, they need to be further amplified by charge amplifiers, and then enter into a computer. The computer records and saves the vibration test data through the related software.

Fig. 5: Real vehicle test

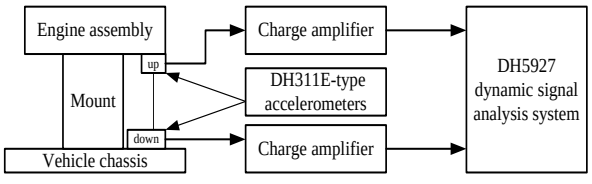

Fig. 6: Vibration response test schematic of mount up and down test point

4.2. Test results

According to the above measure flowchart in Fig. 6, the test results are obtained. Here, vibration acceleration data of the time domain for right mounts up and down test points at normal driving are shown in Table 3, and the corresponding data at normal driving for left mounts are given in Table 4. It should be noted that the sensors which are used in this experiment are three-axis piezoelectric DH311E-type accelerometers. Each measurement direction is shown in Fig. 4, the longitudinal direction stands for the X-axis which is the direction of the vehicle travelling, the lateral direction is the Y-axis, and the vertical one is the Z-axis. In Table 3 and 4, not only the maximum and minimum value of test points are given, but also their RMS values are presented. Here, RMS values of the time domain vibration acceleration signal could be obtained as,

$$a_{RMS} = \sqrt{\frac{1}{N} \sum_{i=1}^{N} a_i^2} \tag{11}$$

Where a RMS refers to the value of root mean square of a set of N acceleration measurement signal (m/s^2), a_i stands for the i^{th} acceleration signal component.

Table 3: Vibration acceleration data of right mounts up and down test point at normal driving(m/s^2)

Dir. Pt.	Right front mount			Right rear mount		
	Max.	Min.	RMS	Max.	Min.	RMS
Z-up	9.122	-14.805	3.927	16.007	-21.384	6.018
Z-down	5.164	1.944	2.927	10.331	-11.722	3.883
X-up	12.430	-12.104	2.841	10.752	-9.934	3.523
X-down	16.144	-12.378	3.726	8.139	-7.633	2.802
Y-up	10.230	-16.160	4.566	9.244	-7.889	3.307
Y-down	5.582	-6.586	2.447	4.038	-4.538	1.904

Table 4: Vibration acceleration data of left mounts up and down test point at normal driving (m/s^2)

Dir. Pt.	Left front mount			Left rear mount		
	Max.	Min.	RMS	Max.	Min.	RMS
Z-up	13.041	-15.021	4.447	17.319	-22.547	6.083
Z-down	16.840	-25.202	6.874	14.216	-16.889	4.459
X-up	14.890	-11.728	3.679	9.742	-14.393	3.872
X-down	12.616	-12.815	3.379	9.397	-11.118	3.055
Y-up	15.665	-15.680	5.031	15.976	-10.352	3.521
Y-down	8.863	-7.193	2.824	5.161	-5.490	2.129

From Table 3 and 4, it could be seen that all the vibration accelerations of the two rear mounts are decreased in three directions. For the right rear mount, the RMS in Z-direction changes from $6.018 m/s^2$ to $3.883 m/s^2$, its absolute reduction is $2.135 m/s^2$ and its relative reduction is 35.5%. At the same time, the RMS value of X-direction for the right rear mount reduces from $3.523 m/s^2$ to $2.802 m/s^2$, the relative decrease is 20.5%, and the Y-direction relative decrease is 42.4%. So, through the contrast of three different directions, the Y-direction vibration-reducing performance of the right rear mount is better than the other directions. Next, the analysis of the left rear mount shows that its RMS value of Z-direction vibration acceleration transforms from $6.083 m/s^2$ to $4.459 m/s^2$, its absolute reduction is $1.624 m/s^2$ and its relative reduction is 26.7%, and the RMS value of X-direction of up and down are 3.872 and

3.055m/s^2 respectively. It is clear that at this time its relative reduction becomes 21.1%, and at last, the relative reduction of Y-direction RMS value is 39.5%. Like the right rear mount, the Y-direction vibration isolation effect of the left rear mount is satisfactory.

Fig. 7 gives the vertical vibration acceleration contrast of left rear mount at normal driving. However, comparative analysis results of acceleration for the two front mounts are different from those for the rear mounts, which could be seen from Table 3 and 4. For the right front mount, the maximum acceleration is along the X-axis while the minimum acceleration occurs on the different up and down test point. The RMS value of Z-direction reduces from 3.927m/s^2 to 2.927m/s^2, its relative reduction is 25.5%. Its Y-direction values also decline to some extent. But its X-direction values don't decrease, the maximum acceleration rises from 12.430 to 16.144m/s^2, the change of minimum value is not obvious, the absolute increase of RMS is equal to 0.885m/s^2. This phenomenon is produced because of the vibration energy coupling of different directions. So the structure parameters of the tubular constrained damping engine mount need to be further optimized. For the left front mount, when the vehicle is working during the normal driving, the X and Y-direction accelerations drop, while the acceleration of Z direction rises, the reason is the same with that of the right front mount.

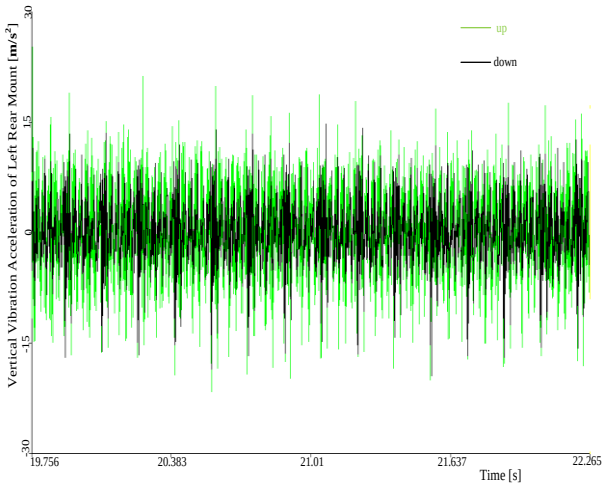

Fig. 7: Vertical vibration acceleration contrast of left rear mount at normal driving

The test data for right and left mounts up and down test points when the engine is running at idle are shown in Table 5 and 6 respectively. At this time, the only vibration source is non-uniform engine rotational speed. From Table 5 and 6, the amplitudes of acceleration for the two rear mounts decrease, in other words, the better vibration isolation performance have been gotten through this design. Through further analysis for the right rear mount, it may be found that the RMS value of Z-direction drops from the 6.002m/s^2 to 3.632m/s^2, its absolute reduction is 2.37m/s^2 and this value is larger than those of the other two directions. The absolute reductions in Z, X and Y-axis for the right rear mount are 39.5%, 27.9% and 35.8%, respectively. For the left rear mount, the RMS in Z-axis changes from 6.010m/s^2 to 4.043m/s^2, and the RMS in X-axis reduces from 3.475 to 2.701m/s^2, the RMS in Y-axis declines from 3.172m/s^2 to 1.938m/s^2, therefore, their absolute reductions in Z, X and Y-axis are 1.967, 0.774 and 1.234m/s^2 and their absolute reductions in Z, X and Y-axis are 32.7%, 22.3% and 38.9%, respectively. For the two front mounts when the engine is at idling, the vibration-isolating effects in some directions are not good. For example, the maximum value of acceleration in X-direction for the right front mount gets from 7.871m/s^2 to 11.451m/s^2 and both the minimum and RMS value don't change smaller. These results are similar with those of the left front mount. Therefore, it further shows that it is necessary and urgent for the next research to optimize the structure parameter of the designed tubular engine mount.

Table 5: Vibration acceleration data of right mounts up and down test point at idle(m/s^2)

Dir. Pt.	Right front mount			Right rear mount		
	Max.	Min.	RMS	Max.	Min.	RMS
Z-up	11.246	-12.119	3.943	16.214	-21.995	6.002
Z-down	2.881	-0.101	0.843	9.470	-11.380	3.632
X-up	7.871	-8.744	2.266	13.590	-10.605	3.382
X-down	11.451	-9.738	3.029	6.412	-6.418	2.439
Y-up	9.268	-11.579	4.348	8.560	-7.096	2.832
Y-down	5.133	-5.792	1.935	4.721	-4.117	1.818

Table 6: Vibration acceleration data of left mounts up and down test point at idle (m/s^2)

Dir. Pt.	Left front mount			Left rear mount		
	Max.	Min.	RMS	Max.	Min.	RMS
Z-up	18.653	-28.004	6.374	16.443	-19.813	6.010
Z-down	10.025	-13.330	4.153	11.542	-15.119	4.043
X-up	9.500	-10.242	3.171	10.636	-13.312	3.475
X-down	10.886	-10.407	2.699	7.181	-8.341	2.701
Y-up	13.514	-16.245	4.664	9.900	-9.931	3.172
Y-down	7.620	-8.679	2.694	5.063	-6.021	1.938

5. Conclusion

A type of tubular constrained damping engine mount is first used in the underground trackless vehicle in order to reduce the vibration level of the vehicle body. This tubular sandwiched engine mount is made of three layers. The material of the middle layer is natural rubber, and the vibration energy is mainly dissipated by the deformation and hysteresis of rubber to achieve the design requirements. To know about the vibration isolation performance of the tubular sandwiched engine mount, the real vehicle test was done. Vibration acceleration data of the time domain for the mounts up and down test points during the normal driving and at idle are given. When the vehicle is operated during the normal driving, the relative reductions of RMS for the right rear mount in Z, X and Y direction are 35.5%, 20.5% and 42.4%, and those for the left rear mount are 26.7%, 21.1% and 39.5%, respectively. When the vehicle is running at idle, the absolute reductions of RMS for right rear mount in Z, X and Y-axis are 39.5%, 27.9% and 35.8%, and those for left rear mount are 32.7%, 22.3% and 38.9%, respectively. However, the RMS for the two front mounts in a certain direction under two different working conditions don't decrease sometimes, this phenomenon is related to the vibration

energy coupling in different directions. The results in this paper are helpful for the further application of tubular sandwiched structure in various vehicles.

ACKNOWLEDGEMENTS:

The authors would like to thank the Research Project Supported by National Natural Science Foundation of China (Grant No. 51405323) for its support.

REFERENCES:

[1] R. Hansen. 2015. Analysis of methodologies for calculating the heat release rates of mining vehicle fires in underground mines, *Fire Safety J.*, 71, 194-216. https://doi.org/10.1016/j.firesaf.2014.11.008.

[2] A.K. Dash, R.M. Bhattcharjeea, P.S. Paul and M. Tikader. 2015. Study and analysis of accidents due to wheeled trackless transportation machinery in indian coal mines - identification of gap in current investigation system, *Proc. Earth and Planetary Sci.*, 11, 539-547. https://doi.org/10.1016/j.proeps.2015.06.056.

[3] A.T. Alisaraei, B. Ghobadian, T.T. Hashjin and S.S. Mohtasebi. 2012. Vibration analysis of a diesel engine using biodiesel and petrodiesel fuel blends, *Fuel*, 102, 414-422. https://doi.org/10.1016/j.fuel.2012.06.109.

[4] Y.H. Yu, S.M. Peelamedu, N.G. Naganathan and R.V. Dukkipati. 2001. Automotive vehicle engine mounting systems: A survey, *J. Dyn. Syst.-T ASME*, 123(6), 186-193.

[5] J. Orivuori, I. Zazas and S. Daley. 2012. Active control of frequency varying disturbances in a diesel engine, *Control Engg. Pract.*, 20, 1206-1219.

[6] M. Östberg, M. Coja and L. Kari. 2013. Dynamic stiffness of hollowed cylindrical rubber vibration isolators - the wave-guide solution, *Int. J. Solids Struct.*, 50, 1791-1811. https://doi.org/10.1016/j.ijsolstr.2013.02.008.

[7] W.C. Flower. 1985. Understanding hydraulic mounts for improved vehicle noise, vibration and ride qualities, *SAE Technical Paper Series*, 850975.

[8] J. Christopherson and G. Nakhaie Jazar. 2006. Dynamic behavior comparison of passive hydraulic engine mounts. Part 1: Mathematical analysis, *J. Sound Vibr.*, 290, 1040-1070. https://doi.org/10.1016/j.jsv.2005.05.008.

[9] T.Q. Truong and K.K. Ahn. 2010. A new type of semi-active hydraulic engine mount using controllable area of inertia track, *J. Sound Vibr.*, 329, 247-260. https://doi.org/10.1016/j.jsv.2009.09.015.

[10] C. Bohn, A. Cortabarria, V.H. Artel and K. Kowalczyk. 2004. Active control of engine-induced vibrations in automotive vehicles using disturbance observer gain scheduling, *Control Engg. Pract.*, 12(8), 1029-1039.

[11] I.L. Ladipo, J.D. Fadly and W.F. Faris. 2016. Characterization of magnetorheological elastomer (MRE) engine mounts, *Materials Today: Proc.*, 3, 411-418. https://doi.org/10.1016/j.matpr.2016.01.029.

[12] J. Cheer and S.J. Elliott. 2016. Active noise control of a diesel generator in a luxury yacht, *Appl. Acoust.*,105, 209-214. https://doi.org/10.1016/j.apacoust.2015.12.007.

[13] S. Prakash, T.G. Renjith Kumar, S. Raja and D. Dwarakanathan. 2016. Active vibration control of a full scale aircraft wing using a reconfigurable controller, *J. Sound Vibr.*, 36, 132-149. https://doi.org/10.1016/j.jsv. 2015.09.010.

[14] S. Daley, F.A. Johnson, J.B. Pearson and R. Dixon. 2004. Active control for marine applications, *Control Engg. Pract.*, 12(4), 465-474.

[15] J. Shen, H.Q. Zhu, M.G. Luo and D.L. Liu. 2016. Numerical simulation of CO distribution discharged by flame-proof vehicle in underground tunnel of coal mine, *J. Loss Prevent Proc.*, 40, 117-121. https://doi.org/10.1016 /j.jlp.2015.12.009.

[16] P. Charles, J.K. Sinha, F. Gu and L. Lidstone. 2009. Detecting the crankshaft torsional vibration of diesel engines for combustion related diagnosis, *J. Sound Vibr.*, 321, 1171-1185. https://doi.org/10.1016/j.jsv.2008.10.024.

[17] M. Hooshang, R. Askari Moghadam and S. AlizadehNia. 2016. Dynamic response simulation and experiment for gamma-type stirling engine, *Renew. Energ.*, 86, 192-205. https://doi.org/10.1016/j.renene.2015.08.018.